# Mutant Kras-induced expression of ICAM-1 in pancreatic acinar cells causes attraction of macrophages to expedite the formation of precancerous lesions

**Geou-Yarh Liou**[1], **Heike Döppler**[1], **Brian Necela**[1], **Brandy Edenfield**[1], **Lizhi Zhang**[2], **David W. Dawson**[3], and **Peter Storz**[1]

[1]Department of Cancer Biology, Mayo Clinic, Jacksonville, FL, USA

[2]Department of Laboratory Medicine & Pathology, Mayo Clinic, Rochester, MN, USA

[3]Department of Pathology & Laboratory Medicine, David Geffen School of Medicine at UCLA, Los Angeles, CA, USA

## Abstract

Desmoplasia and an inflammatory environment are defining features of pancreatic cancer. Unclear is how pancreatic cells that undergo oncogenic transformation can crosstalk with immune cells and how this contributes to the development of pancreatic lesions. Here we demonstrate that pancreatic acinar cells expressing mutant Kras can expedite their transformation to a duct-like phenotype by inducing local inflammation. Specifically, we show that Kras$^{G12D}$ induces the expression of intercellular adhesion molecule-1 (ICAM-1), which serves as chemoattractant for macrophages. Infiltrating macrophages amplify the formation of Kras$^{G12D}$-caused abnormal pancreatic structures by re-modulating the extracellular matrix and providing cytokines such as tumor necrosis factor (TNF). Depletion of macrophages or treatment with a neutralizing antibody for ICAM-1 in mice expressing oncogenic Kras under an acinar cell-specific promoter both resulted in a decreased formation of abnormal structures and decreased progression of ADM to PanIN lesions.

### Keywords

pancreas; PanINs; precancerous lesions; Kras; macrophage

## INTRODUCTION

Oncogenic Kras mutations drive metaplasia of pancreatic acinar cells to a highly-proliferative duct-like cell type, which is the precursor for precancerous pancreatic intraepithelial neoplastic lesions (PanINs) (1, 2). While such Kras-induced acinar-to-ductal metaplasia (ADM) can be seen as an initial event that leads to development of pancreatic lesions, additional mutations (i.e. loss of the tumor suppressor genes p16[INK4A], p53 and SMAD4) are required for further progression to pancreatic cancer (3). Recent evidence also suggests that alterations in the pancreatic microenvironment are key factors for further development from precancerous lesion to pancreatic ductal adenocarcinoma (PDA). For example, it was demonstrated that caerulein-induced release of digestive enzymes and subsequent pancreatic inflammation in Kras[G12D]-expressing mice accelerates the development of PDA (4). Similarly, a high fat diet in Kras[G12D]-expressing mice dramatically accelerates PDA by causing pancreatic inflammation and macrophage infiltration (5). Consequently, in humans environmental risk factors for the development of pancreatic cancers are pancreatitis, and inducers of inflammatory responses such as obesity and smoking (6, 7).

While a functional link between inflammation and oncogenic Kras for progression of PDA was demonstrated in above mouse models, inflammation may not only accelerate Kras-driven pancreatic cancer, but also initiate the ADM process. For example, it was recently shown that depletion of macrophages in a mouse model for acute pancreatitis completely protected acinar cells from undergoing ADM, resulting in a protection of the pancreas from injury (8). Mechanistic insight of how inflammation contributes to changes in the pancreas microenvironment was provided by demonstrating that macrophages can secret cytokines that drive ADM. These include TNF, RANTES (8) and HB-EGF (9). However, while the contribution of Kras-initiated signaling pathways that induce ADM is relatively well defined (i.e. MAPK activation, cooperation with EGFR signaling) (10), the signaling crosstalk between Kras-expressing pancreatic cells and cells of the microenvironment is just getting investigated (8, 9, 11, 12). Specifically, whether Kras[G12D] expression in acinar cells can initiate signaling pathways that facilitate local inflammation is unknown.

Here we report that oncogenic Kras mutations in pancreatic acinar cells induce the expression of intercellular adhesion molecule-1 (ICAM-1). We show that ICAM-1 can act as a chemoattractant for macrophages. Attracted macrophages release matrix degrading enzymes including matrix metalloproteinase 9 (MMP9), as well as cytokines such as TNF that synergize with Kras mutations to drive acinar cell metaplasia. We demonstrate that depleting macrophages or neutralizing ICAM-1 in p48[cre];Kras[G12D]-expressing mice dampens the development of precancerous lesions. In summary, our data for the first time demonstrate that Kras[G12D]-expressing acinar cells can expedite their transformation to a duct-like phenotype by inducing local inflammation and macrophage infiltration. Overall, we provide a mechanism of how oncogenic Kras mutations and inflammatory microenvironment function synergistically to drive earliest abnormal pancreatic structures that precede PDA.

# RESULTS

## Macrophages contribute to Kras$^{G12D}$-induced formation and progression of pancreatic lesions

Pancreatitis and macrophage infiltration have been associated with faster progression of pancreatic lesion to tumors (4, 13). In order to test if macrophages can contribute to the initiation of pancreatic cancer, we utilized the p48$^{cre}$;LSL-Kras$^{G12D}$ animal model, in which an oncogenic mutant of Kras is expressed under an acinar cell-specific promoter, and depleted macrophages by treatment with Gadolinium (III) chloride (GdCl$_3$). Treatment with GdCl$_3$ (treatment schedule shown in Supplemental Fig. S1A) significantly decreased the presence of macrophages in the Kras$^{G12D}$-expressing pancreata (Fig. 1A), but had no effects on the presence of CD3-positive T-cells or neutrophils (Supplemental Fig. S1B). While PBS-treated p48$^{cre}$;LSL-Kras$^{G12D}$ mice showed ADM and PanIN formation, the formation of these abnormal structures was significantly-reduced in absence of macrophages (Fig. 1A and Supplemental Fig. S1C). Quantitative analysis of pancreata showed that when macrophages were depleted overall number of lesions (abnormal structures) were decreased approximately 50% (Fig. 1B). Division of abnormal structures into regions of isolated ADM, ADM-PanIN transition areas or PanIN lesions suggested a slower progression of Kras-caused oncogenesis when macrophages were absent. For example, in absence of macrophages isolated ADM areas increased from 25% to 36% and total PanIN lesions decreased from 48% to 38%. Within these PanIN lesions the occurrence of PanIN1A/1B increased from 77% to 89% and PanIN2/3 lesions decreased from 23% to 11%. Overall, this suggests that macrophages can contribute to the progression of ADM to PanINs. This is supported by an increased occurrence of macrophages in ADM regions, as compared to established PanIN lesions (Fig. 1C).

## Mutant Kras induces expression of ICAM-1 in acinar cells

We next determined if mutant Kras in acinar cells can induce the expression of chemoattractants for immune cells. Therefore, we infected primary mouse acinar cells with lentivirus carrying an oncogenic Kras (Kras$^{G12V}$) mutant or a control virus and then tested for expression of different chemoattractants. These included CXCL11 (chemoattractant for activated T-cells), CXCL10 (chemoattractant for T-cells, NK cells, dendritic cells and monocytes/macrophages) and ICAM-1 (chemoattractant for leukocytes). While expression of mutant Kras had little effects on CXCL10 and CXCL11 expression, the expression of mRNA for ICAM1 was increased approximately 100-fold as compared to control cells (Fig. 2A). At the same time the expression of EGFL7, a molecule previously-described as inhibitor of ICAM1 expression (14) was significantly decreased. Increased ICAM-1 mRNA levels translated to increased levels of full-length protein, as judged by Western blotting (Fig. 2B). Interestingly, we also detected slightly increasing levels of soluble ICAM-1 (sICAM-1) in the supernatant of 3D organoid cultures undergoing Kras$^{G12V}$-driven ADM. During transdifferentiation of cells sICAM-1 levels increased from approximately 0.1 –/+0.044 ng/ml at the day of seeding in 3D culture to 0.36 –/+ 0.035 ng/ml at day 5 of Kras$^{G12V}$ expression (Fig. 2C).

Accordingly to Kras-driven expression of ICAM-1 in acinar cell 3D organoid culture, ICAM-1 expression also was detected in regions of ADM in p48[cre];LSL-Kras[G12D], but not in control mice (Fig. 2D). This correlated with presence of macrophages in these regions as determined by F4/80 staining. Regions of ADM also showed an increase of cytokeratin-19, a marker for duct-like cells (Supplemental Fig. S2A). Interestingly, further progressed PanIN lesions in the same samples did show significantly-less ICAM-1 expression and less macrophage infiltration in these areas (Supplemental Fig. S2B). Since regions of PanIN and PDA also contain microvessels (15) that could contribute to occurrence of ICAM-1 in the pancreas *in vivo*, we performed an additional experiment to demonstrate that Kras[G12D]-expressing acinar cells indeed upregulate ICAM-1. Therefore, we isolated acinar cells from p48[cre];Kras[G12D] mice (Kras[G12D] expression only in acinar cells) or control mice and tested if they express ICAM-1. Increased ICAM-1 expression was detected in acinar cells from p48[cre];Kras[G12D] mice as compared to normal acinar cells, indicating that acinar cells indeed are the source of ICAM-1 (Fig. 2E). Moreover, an immunohistochemical analysis of regions of ADM in p48[cre];Kras[G12D] mice for endothelial cells (anti-CD31 as a marker) did not indicate significant presence of vessels in these regions, indicating that microvascularization may occur at a later time during tumor development (Supplemental Fig. S3A).

Similarly to data obtained with above genetic mouse model, in human samples ICAM-1 expression was detected by IHC in regions of ADM, but not in adjacent "normal" tissue or PanIN lesions of types 1A, 1B or 2 (Fig. 2F, and Supplemental Fig. S3B). The exclusive presence in regions of ADM in samples of human origin or mouse genetic models indicates that the expression of ICAM-1 is an initial event that may contribute to the ADM process, but may be less needed during the progression of PanINs.

## Kras[G12D]-caused expression of ICAM-1 serves as a chemoattractant for macrophages

ICAM-1, when expressed in endothelial cells, was shown to promote neutrophil adhesion and trans-endothelial migration (16, 17). We next tested if ICAM-1 also can act as an attractant for macrophages. In an initial experiment, to test if cells that express ICAM-1 can attract macrophages, we generated HeLa cells stably-expressing GFP-tagged full-length transmembrane ICAM-1 and co-cultured these cells in spatial separation with Raw264.7 macrophage cells stained with a life cell dye. Control cells expressed GFP, but neither ICAM-1 mRNA nor endogenous or ectopic protein was detected (Supplemental Figures S4A, S4B). After removal of the separation barrier, we observed that expression of GFP-tagged ICAM-1 led to attraction of macrophages (Fig. 3A). We then analyzed the supernatant of ICAM-1 expressing cells for the soluble version of this protein (sICAM-1) by ELISA, and detected sICAM-1 at 2.599 −/+ 0.422 ng/ml.

Although above experiment is a proof of principle to show that macrophages can be attracted by cells expressing ICAM-1, two questions remained unanswered. First, can the secreted soluble ICAM-1 contribute to such chemoattraction, and second, which polarized phenotype of macrophage (M1 or M2) is attracted? We found that Raw264.7 cells migrate towards recombinant soluble ICAM-1 in Transwell assays (Supplemental Fig. 4C). However, this cell line expresses markers for both M1 (i.e. positive for iNOS) and M2 (i.e. positive for Ym1) macrophages (Supplemental Fig. 4D), and we were not able to obtain

clean polarization to one of these phenotypes after LPS + IFNγ or IL-4 stimulation (data not shown). Therefore, we decided to use freshly-isolated primary mouse macrophages. After treatment with LPS + IFNγ or IL-4, we observed ideal M1 or M2 polarization, respectively (Supplemental Figs. S4E, S4F). Freshly-isolated mouse primary macrophages as well as fully-polarized M1 macrophages migrated towards recombinant sICAM1 in a dose-dependent manner in Transwell assays. M2-polarized macrophages generally showed higher motility, but were not attracted by sICAM-1 (Fig. 3B, 3C).

Eventually, to demonstrate that expression of mutant Kras in primary acinar cells can induce the attraction of primary macrophages, we isolated acinar cells from LSL-Kras$^{G12D}$ mice and induced Kras$^{G12D}$ expression by infection with adeno-cre or control virus (adeno-null). We then determined the migration of freshly-isolated or polarized (M1 or M2) primary mouse macrophages towards the Kras$^{G12D}$-expressing or control acinar cells in a transwell assay. We found that chemoattraction of freshly-isolated or M1-polarized macrophages by acinar cells expressing mutant Kras was significantly increased, while M2-polarized macrophages although highly motile were not specifically attracted (Figs. 3D, 3E). To show that Kras$^{G12D}$-caused chemoattraction is dependent on ICAM-1 expression we added an ICAM-1 neutralizing antibody (NAB) to the assay (columns 3 and 4 in Figs. 3D, 3E) - and this completely blocked Kras$^{G12D}$-induced chemoattraction of M1 macrophages. In summary, our data show that acinar cells expressing an oncogenic allele of Kras can facilitate the attraction of primary macrophages of the M1 phenotype via ICAM-1 *in vitro*.

## Blocking ICAM-1 with a neutralization antibody decreases macrophage infiltration and Kras-caused abnormal structures *in vivo*

We next tested if blocking macrophage attraction with an ICAM-1 neutralization antibody is sufficient for decreasing or blocking Kras-caused formation of abnormal pancreatic structures *in vivo*. Therefore, we treated p48$^{cre}$;LSL-Kras$^{G12D}$ mice with ICAM-1 NAB over a time period of 11 weeks, starting at an age of 3 weeks (treatment schedule shown in Supplemental Fig. S5A). For controls, mice were either treated with PBS (vehicle) or an isotype-matched antibody (Control AB). At the endpoint (week 14) we found that neutralization of ICAM-1 not only led to a drastic decrease of macrophage infiltration into the pancreas, but also to a significant reduction of abnormal lesion structures (Fig. 3F; additional controls and IHC for the PanIN marker Claudin-18 are shown in Supplemental Fig. S5B). Results from a basic complete blood count test suggested that administering repeated doses of an anti-ICAM-1 antibody had no effects on generalized immune reactions in mice (Supplemental Fig. S5C). Moreover, in our hand, control mice treated with ICAM-1 NAB did not show any presence of immune cells in the pancreas. However, in the Kras$^{G12D}$-expressing pancreas we clearly show that while macrophage attraction is blocked by an ICAM-1 NAB, Ly6B.2-positive cells (neutrophils) and CD3-positive cells (T-cells) are still present (Supplemental Figs. S5B and S5D).

Comparable to the effects we had observed after ablation of macrophages in Fig. 1, we found that neutralization of ICAM-1 led to an increase in regions of isolated ADM (from 23% to 32 %) and a decrease of total PanIN lesions from 47% to 36% (Fig. 3G). Within these PanIN lesions the occurrence of PanIN1A/1B increased from 80% to 89% and

PanIN2/3 lesions decreased from 20% to 11%. Overall, neutralization of ICAM-1 had almost identical effects on the composition of abnormal structures than depletion of macrophages.

### Macrophages-secreted cytokines and proteases contribute to ADM

We recently have shown that in an inflammatory environment in the pancreas infiltrating macrophages secrete a panel of cytokines of which some can initiate acinar-to-ductal metaplasia (8). One major driver of macrophage-induced ADM we had identified is TNF (8). Since Kras$^{G12D}$-expressing acinar cells also attract macrophages, we next tested if this correlates with presence of TNF in regions of ADM. We found that in p48$^{cre}$; Kras$^{G12D}$ mice in regions of ADM the presence of TNF and macrophages correlated and both did not occur when ICAM-1 expression was blocked with the neutralization antibody (Fig. 4A). Then, to directly determine if TNF can contribute to the Kras$^{G12D}$-driven ADM process we performed a 3D explant organoid assay. Therefore, we isolated primary acinar cells from LSL-Kras$^{G12D}$ mice and induced Kras$^{G12D}$ expression by transduction of cre recombinase with an adeno-cre virus (or adeno-null as control). Then acinar cells were seeded in 3D collagen culture and treated with TNF or control as indicated (Fig. 4B). At day 5, ADM events were determined. Both Kras$^{G12D}$ mutation and TNF acted synergistically to increase the number of ADM events (ADM event = metaplasia of acinar cells of duct-like cells) as well as size of duct-like structure formed.

Since macrophages also are known for their ability to secrete proteases that degrade extracellular matrix we next tested if regions of ADM showed increased protease activities. Therefore, we first performed an *in situ* zymography of pancreata of p48$^{cre}$;LSL-Kras$^{G12D}$ mice and found increased ECM degradation in ADM and PanIN regions (Fig. 4C). This may be due to increased activities of matrix metalloproteinases as well as other proteases such as members of the ADAM family (8, 10). However, in 3D explant organoid assays ADM events could be significantly-blocked with the matrix metalloproteinase inhibitor GM6001 suggesting a major role of MMPs (Supplemental Fig. S6). Since in experimental pancreatitis MMP9 was shown to be a major contributor to the ADM process (8) we next investigated if appearance of macrophages in regions of ADM correlates with presence of MMP9. We found MMP9 expression co-localizing with macrophages in regions of ADM in p48$^{cre}$;LSL-Kras$^{G12D}$ mice, but not in control mice or in p48$^{cre}$;LSL-Kras$^{G12D}$ mice in which we had depleted macrophages by treatment with GdCl$_3$ (Fig. 4D). Taken together, our data indicate that M1 macrophage-secreted cytokines such as TNF as well as proteases including MMP9 can contribute to mutant Kras-driven ADM. Fig. 4E provides a model of how the interaction of acini and macrophages may occur to promote acinar-cell metaplasia to a duct-like phenotype that is believed to be the precursor of PanIN lesions.

## DISCUSSION

Activating Kras mutations have been long-recognized as the drivers of pancreatic intraepithelial lesions (18). When expressed in mice under pancreatic cell-specific (i.e. PDX1 or Pft1a/p48) promoters, Kras$^{G12D}$ induces ADM and formation of PanINs (1, 19). However, expression of Kras$^{G12D}$ does not lead to all acinar cells undergoing ADM

simultaneously, and pancreata of mice show patchy regions of isolated ADM, ADM/PanIN transition areas as well as progressed lesions (1, 19). A possible explanation is that in order to drive transformation, Kras[G12D]-expressing cells need to interact with cells of the pancreatic microenvironment, including pancreatic stellate cells or infiltrating immune cells (13, 20, 21). However, direct experimental evidence to such a crosstalk for these initial processes was lacking. We here show that attraction of macrophages and microinflammation caused by expression of oncogenic Kras in acinar cells, is a necessary event to drive the formation of precancerous lesions (Fig. 1). Our data suggest that macrophage infiltration predominantly occurs in regions of ADM, but less in the PanIN stage, indicating importance for macrophage-released factors in the initiation of acinar cell transdifferentiation. Different roles have been demonstrated for M1 and M2 macrophages (22). Both subtypes can be detected in pancreata of p48cre;LSL-Kras[G12D] mice (data not shown), but their relative contribution to Kras-driven ADM at this point is unclear. Because M1 macrophages are attracted by ICAM-1 (Fig. 3) and because we observe presence of TNF after macrophage attraction (Fig. 4A), we predict that this subtype has a predominant role in driving ADM. However, since M2 macrophages have been shown to activate stellate cells, it is likely that they also contribute via other mechanisms to a crosstalk between multiple cell types to drive ADM.

TNF in M1 macrophages is a NF-κB target gene (23). Activation of this transcription factor could be achieved during M1 polarization via IFNγ and LPS (24), which both have been shown to upregulate NF-κB signaling (25, 26). Another possibility is that M1 macrophages once attracted to the acinar cell clusters physically interact with ICAM-1 on acinar cells via MUC-1, which also can activate NF-κB (27). In addition, NF-κB may also participate in Kras-induced expression of ICAM-1 in acinar cells. It was shown that ICAM-1 expression is regulated by NF-κB1 (28); and NF-κB1 can be activated by oncogenic Kras and also amplify Ras activity in pancreatic cancer cells (29, 30).

ICAM-1 is a transmembrane protein that can be converted into a soluble protein (sICAM-1) by shedding (31), and thus can act as a chemoattractant. Acinar cells express several proteinases that could drive this process. It was shown that matrix metalloproteinases (MMPs) can facilitate the formation of soluble ICAM-1 (32). MMP3 has been demonstrated to be up-regulated during ADM and to stimulate immune cell infiltration, priming the microenvironment for early tumor development (33). It is possible that MMP3 to some extend is responsible for the generation of sICAM-1. Another proteinase that is upregulated by oncogenic Kras is ADAM17 (34), which has been reported to produce soluble ICAM-1 (35). Increased circulating levels of soluble ICAM-1 can be detected in pancreatic cystic fluid of pancreatitis patients suggesting it as a potential marker for presence of pancreatic disease (36).

The function of ICAM1 in the development and progression of PDA so far was not well understood. By showing that it is produced by acinar cells that express oncogenic Kras, we provide a role for ICAM-1 in the initiation of pancreatic cancer by attracting M1 macrophages. Our data also show that only a fraction of the ICAM-1 produced by acinar cells is soluble. Expression of full-length (transmembrane) ICAM-1 in acinar cells may also have additional functions such as acting as antagonist to β2 integrin to loosen cell-matrix

connections and enhance ADM. Another possible function is to acts as a receptor for M1 macrophage attachment via interaction with the leukocyte adhesion protein LFA-1 (leukocyte function-associated antigen-1) and MUC-1. At this point it is unclear which surface receptors macrophages use to chemo-detect ICAM-1, and if a direct contact between both cell types is needed to drive the ADM process. For example, it is also possible that pancreatic stellate cells are involved as an intermediate cell type in this crosstalk (20, 21). Since ICAM-1 and sICAM-1 can have antagonistic effects on the tight junctions (31), they also could act as an autocrine mechanism to affect neighboring cells and to alter the structures of acinar cell clusters.

While our data suggests a role of ICAM-1 expression by acinar cells as a driving force in tumor-initiating events, the role of ICAM-1 expression in the actual cancer is less clear. In pancreatic cancer cell lines it was shown that ICAM-1 expression was significantly-increased as compared to normal pancreatic cells (37). Moreover, the ICAM-1 expression status was linked to the poor prognosis of pancreatic cancer (38). Although our data show that in human tissue ICAM-1 expression mainly occurs in regions of ADM and decreases in regions of PanINs (Fig. 2F), we confirmed that it is re-expressed in human pancreatic cancer (Supplemental Figure S3C). The re-expression in established adenocarcinoma may be due to increased vascularization (15), and be unrelated to acinar-cell produced ICAM-1.

Understanding the crosstalk between pancreatic cells expressing oncogenic Kras mutations and the pancreas microenvironment is of importance to develop targeted strategies for this cancer, including immunotherapy to increase responsiveness of the adaptive immune system (39). Our findings that macrophages are attracted by Kras-expressing acinar cells, and directly contribute to their transdifferentiation by providing inflammatory cytokines or proteases could be an additional angle to target the microenvironment leading to tumor formation, but also to develop biomarkers for early detection. For example, ICAM-1 levels in the pancreatic juice in combination with markers for advanced PanINs (40) could be predictive markers for presence of pre-neoplastic lesions. After prediction of the potential of patients to develop pancreatic cancer the use of neutralizing antibodies may be a way to prevent progression of precancerous lesions. ICAM-1 blocking antibodies have been tested for different disease models and species *in vivo*. Most studies in which ICAM-1 blocking antibodies were used to mitigate inflammation or prevent migration of cells to inflammatory lesions have been performed in rats using mouse monoclonal IgG antibodies (41, 42). The ICAM-1 blocking antibody we used is a monoclonal IgG made in hamster, which previously was used for studies to diminish macrophage recruitment to atherosclerotic plaques (43). With our animal studies (Fig. 3F and Supplemental Fig. S5) we provide a *proof-of-principle* experiment for the use of such blocking antibodies for clinical use in humans. One of these, Enlimomab, has already been developed for treatment of ischemic stroke, refractory rheumatoid arthritis, kidney and liver allograft transplantations (44).

## METHODS

### Cell lines, antibodies, viral constructs and reagents

Raw264.7 and HeLa were obtained from American Type Culture Collection (ATCC, Manassas, VA). Cells were not further authenticated, but have been passaged in the

laboratory for fewer than 6 months. All cell lines were maintained in DMEM (high glucose) with 10% FBS and 100 U/ml penicillin/streptomycin in a 37 °C incubator supplemented with 5% $CO_2$. For HeLa cell lines stably expressing GFP or full-length transmembrane GFP-ICAM-1, cells were infected with lentivirus (MOI of 5) and 48 hours post infection selected using 5 μg/ml Blasticidin (Invitrogen, Carlsbad, CA) for 10 days and then additionally-selected by FACS analysis. Anti-CD3, anti-F4/80, anti-iNOS, anti-MMP9 and anti-hICAM-1 (used for IHC of human samples) antibodies were from Abcam (Cambridge, MA), anti-mICAM1 (used for IHC of mouse samples) from R&D Systems (Minneapolis MN), anti-Ym1 from Stemcell Technologies (Vancouver, Canada), Ly6B.2 antibody from AbDSerotec (Raleigh, NC), anti-claudin-18 from Invitrogen, anti-amylase from Sigma-Aldrich (St Louis, MO), anti-GFP, anti-CD31 and anti-cytokeratin-19 from Santa Cruz Biotechnology (Dallas, TX). The neutralizing monoclonal hamster IgG antibody (NAB) for mICAM-1 used in the animal experiments was from Thermo Scientific (Waltham, MA); an isotype-specific control antibody was from BD Pharmingen (Franklin Lakes, NJ). Adeno-cre and Adeno-null (empty vector, control) adenovirus was purchased from Vector Biolabs (Philadelphia, PA). pLenti6.3/V5-GFP-ICAM-1 was generated by cloning human ICAM-1 first into pEGFP-N1 using BamHI and EcoRI sites and the following primers: 5'-GAATTCATGGCTCCCAGCAGC-3' and 5'-GGATCCAAGGGAGGCGTGGCTTGTG-3'. GFP-ICAM-1 was then amplified by PCR using 5'-GAATTCATGGCTCCCAGCAGC-3' and 5'-CCGCTCGAGTTACTTGTACAGCTCGTC-3' as primers; and the fragment was inserted into pLenti6.5/V5-TOPO through TOPO cloning using the TOPO cloning kit from Invitrogen. Recombinant mouse soluble ICAM-1 was purchased from Sino Biological Inc. (Beijing, P.R. China), recombinant mouse TNFα, recombinant mouse IL-4, and recombinant mouse IFNγ were from PeproTech (Rocky Hill, NJ). Lipopolysaccharide (LPS), DAPI, gadolinium chloride hexahydrate and dexamethasone were from Sigma-Aldrich. DQ-gelatin was from Invitrogen, agarose from Lonza (Walkersville, MD). Soybean trypsin inhibitor, collagenase I and GM6001 were from EMD Millipore (Billerica, MA). Rat tail collagen I was from BD Biosciences (San Jose, CA).

### Animals and treatments

BALB/c mice for isolation of primary pancreatic acinar cells or primary macrophages were purchased from Harlan Laboratories (Tampa, FL). *Ptf1a/p48$^{Cre/+}$* and *LSL-Kras$^{G12D/+}$* mouse strains and genotyping of mice have been described previously (45–47). To deplete macrophages, mice at 7 weeks of age were intravenously injected with GdCl$_3$ at a dose of 10 mg/kg or phosphate-buffered saline solution as control vehicle every 2 days for 1 week. This was repeated at week 10. At week 13 mice were sacrificed and tissues harvested (see time line Supplemental Figure S1A). To neutralize ICAM-1 *in vivo*, 3 week old mice were intraperitoneally injected with ICAM-1 NAB (or isotype-specific control antibody) at a dose of 2 mg/kg or vehicle every other day for 11 weeks (see time line Supplemental Figure S5B). All animal experiments were approved by the Mayo Clinic IACUC committee and were performed in accordance with relevant institutional and national guidelines and regulations.

## Human pancreatic tissue samples

All patient tissues were obtained in accordance with institutional guidelines and prior institutional review board approval. Tissue microarrays of patient-matched normal pancreas, PanIN and pancreatic adenocarcinoma were constructed from archival materials in the University of California, Los Angeles (UCLA) Department of Pathology and Laboratory Medicine archives, representing patients who underwent gross resection of tumor at UCLA Medical Center between 1987 and 2005. TMA construction was supported by a seed grant from the Hirshberg Foundation for Pancreatic Cancer Research.

## DAB immunohistochemistry and immunofluorescence of tissues

Slides were deparaffinized (one hour, 60° C), de-waxed in xylene (five times for four minutes) and gradually rehydrated with ethanol (100%, 95%, 75%, each two times for three minutes). The rehydrated samples were rinsed in water and subjected to antigen retrieval in 10 mM sodium citrate buffer (pH 6.0). Slides were treated with 3% $H_2O_2$ (five minutes) to reduce endogenous peroxidase activity, washed with PBS containing 0.5% Tween 20, and blocked with protein block serum-free solution (DAKO, Carpinteria, CA) for five minutes at room temperature. Samples were stained with H&E, alcian blue. **(i)** For DAB immunohistochemistry, anti-F4/80 antibody (1:200), anti-Ly6B.2 (1:3000), anti-CD3 (1:200), anti-claudin-18 (1:500), anti-CD31 (1:100), anti-hICAM-1 (1:100) or anti-mICAM-1 (1:8000) in Antibody Diluent Background Reducing Solution (DAKO) and visualized using the EnVision Plus Anti-Rabbit Labelled Polymer Kit (DAKO) according to the manufacturer's instructions for the rabbit antibodies. For the rat antibodies, the Rat-on-Mouse Kit was used (Biocare Medical, Concord, CA). Images were captured using the ScanScope XT scanner and ImageScope software (Aperio, Vista, CA). **(ii)** Immunofluorescence: Sections were subjected to immunofluorescence staining as previously described (8) using anti-amylase (1:300), anti-cytokeratin-19 (1:100), anti-F4/80 (1:200), anti-MMP9 (1:1000), anti-TNFα (1:200) or anti-ICAM1 (1:8000; R&D Systems) in Antibody Diluent Background Reducing solution (Dako) at 4°C, overnight. After 3 washes with PBS containing 0.05% Tween-20, appropriate Alexa Fluor 488, 594 or 633 labeled secondary antibodies from Invitrogen (Grand Island, NY) at a 1:500 dilution were added (RT, 1 hour). DAPI (final concentration 125 μg/ml) was added for 15 minutes after samples were incubated with the secondary antibodies. Fluoromount-G (Southern Biotech, Birmingham, AL) or LabVision PermaFluor (Thermo Scientific) was used as mounting and imaging medium. Images were captured by a fluorescent scanner (ScanScope FL, Aperio) with consistent exposure time and processed using ImageScope software (Aperio).

### *In situ* zymography

This method was described in detail in (48). In brief, frozen pancreas tissue sections (8 μm) were air dried for 10 minutes. DQ-gelatin (0.05 mg/ml)/agarose (1%)/DAPI (1μg/ml) mixture in PBS was added on top of the tissue section and covered with a coverslip. After gelling for 5 minutes at 4 °C, the slides were left at RT for 1 hour and fluorescence was detected with using a fluorescent microscope (IX71; Olympus) and filters for FITC and DAPI.

## Isolation and polarization of primary macrophages

Primary murine macrophages were isolated as previously described (8). In brief, mice were intraperitoneally injected with 2 ml of 5% aged thioglycollate solution. At day five after injection, peritoneal macrophages were collected through a single injection of 10 ml RPMI-1640 containing 10% FBS into the peritoneal cavity and subsequent withdrawal. The peritoneal exudate was centrifuged and washed with RPMI-1640 media containing 10% FBS before plating onto tissue culture dishes. After one hour in a 37 °C incubator supplemented with 5% $CO_2$, cells were vigorously washed with PBS for three times to remove non-adherent macrophages. Polarization of freshly-isolated macrophages to a M1 phenotype was induced by adding 10 ng/ml LPS and 20 ng/ml murine IFNγ; and polarization to a M2 phenotype by adding 20 ng/ml murine IL-4 to the media for 24 hours. Polarization for each experiment was controlled by immunofluorescence analysis of cells for iNOS and Ym1 expression (method described in Supplemental Methods section). Only cell populations were used for experiments that were fully polarized (i.e. M1 = iNOS positive/Ym1 negative; or M2 = iNOS negative/Ym1 positive).

## Isolation of pancreatic acinar cells

The procedure to isolate primary pancreatic acinar cells was described in detail previously (8, 49, 50). In brief, the pancreas was removed, washed twice with ice-cold HBSS media, minced into 1 – 5 mm pieces and digested with collagenase I (37 °C, shaker). The collagen digestion was stopped by addition of an equal volume of ice-cold HBSS media containing 5% FBS. The digested pancreatic pieces were washed twice with HBSS media containing 5% FBS, pipetted through a 500 μm mesh, and then a 105 μm mesh. The supernatant of this cell suspension containing acinar cells was dropwise added to the top of 20 ml HBSS containing 30% FBS. Acinar cells were then pelleted (1000 rpm, two minutes, at 4 °C) and re-suspended in 10 ml Waymouth complete media (1% FBS, 0.1 mg/ml trypsin inhibitor, 1 μg/ml dexamethasone).

## 3D organoid explant culture of primary pancreatic acinar cells

This method was described in detail before (8, 49). In short, cell culture plates were coated with collagen I in Waymouth media without supplements. Freshly isolated primary pancreatic acinar cells from wildtype or LSL-Kras[G12D] mice were added as a mixture with collagen I/Waymouth media on the top of this layer (3D on-top method). Further, Waymouth complete media was added on top of the cell/gel mixture, replaced the following day and then every other day. To express proteins using adenovirus, acinar cells were infected with adenovirus of interest and incubated for three to five hours before embedding in the collagen I/Waymouth media mixture. At day five numbers of ducts in three random fields each sample were determined and photos were taken to document structures.

## Chemoattraction assays

Chemoattraction assays using spatially separated cells in co-culture: HeLa cell pools stably-expressing GFP or GFP-ICAM-1 were generated by infection with lentivirus harboring GFP or GFP-ICAM-1 followed by selection with puromycin. Raw264.7 cells were *in vivo* labeled using Vybrant DiI (Invitrogen). Cells were plated in an ibidi removable 2 well silicone

culture insert that was placed in a cell culture μ-Dish (ibidi, Verona, WI). 24 hours after seeding the culture inserts were carefully removed. After 24 hours, migration of macrophages towards HeLa-GFP or HeLa-GFP-ICAM-1 cells was assessed by fluorescent microscopy (IX71; Olympus). Chemoattraction assays using Transwell plates: Raw264.7 or primary mouse macrophages cells were *in vivo* labeled using Vybrant DiO (Invitrogen). $10^5$ cells were suspended in serum-free DMEM media and placed in the insert of a transwell plate (5 μm pores; polycarbonate membrane). Dependent on the experiment, either mICAM-1 in serum-free DMEM media, or primary pancreatic acinar cells from a LSL-Kras$^{G12D/+}$ mouse infected with null/control or cre-expressing adenovirus in serum-free DMEM media were added to the bottom wells of the transwell plate. Where indicated the ICAM-1 NAB at a final concentration of 3 μg/ml was added to the bottom wells. Triplicates were used for each condition. After 16 hours macrophages migrated through the pores were visualized using a fluorescent microscope (IX71; Olympus). Five fields per sample were randomly chosen and counted.

### Detection of soluble ICAM-1 (sICAM-1) using ELISA

Supernatants of cell culture media were collected and the concentration of sICAM-1 was determined using human or mouse ICAM-1 ELISA kits from R&D Systems. Assays were performed according to manufacturer's instructions.

### RNA Isolation and quantitative PCR

Cells were harvested from explant 3D collagen culture by digestion in a 1 mg/ml collagenase solution at 37 °C for 30 minutes on a shaker. Cells were washed once with HBSS and twice with PBS and total RNA isolation was performed using the miRCURY™ RNA isolation kit (Exiqon, Woburn, MA) and the TURBO DNA-free kit (Ambion, Austin, TX) to eliminate residual genomic DNA. The level of mRNA of interest was assessed using a two-step quantitative reverse transcriptase-mediated real-time PCR (qPCR) method. Equal amount of total RNA was converted to cDNA by the high capacity cDNA reverse transcriptase kit (Applied Biosystems, Bedford, MA). Quantitative PCR was performed in a 7900HT Fast real-time thermocycler (Applied Biosystems) using the TaqMan Universal PCR master mix (Applied Biosystems) with probe/primer sets and the following thermocycler program: 95 °C for 20 seconds; 40 cycles of 95 °C for one second and 60 °C for 20 seconds. All probe/primer sets were purchased from Applied Biosystems (Mm00516023_m1 for mouse ICAM-1, Hs00164932_s1 for human ICAM-1, Mm00618004_m1 for EGFL7, Mm00445235_m1 for CXCL10, Mm00444662_m1 for CXCL11). The amplification data were collected by a Prism 7900 sequence detector and analyzed with Sequence Detection System software (Applied Biosystems). Data were normalized to murine GAPDH, and mRNA abundance was calculated using the $C_T$ method.

### Statistical analysis

Data are presented as means ± SD. P-values were acquired with the Student's *t* test using Prism (GraphPad Software), and $p < 0.05$ is considered statistically significant.

## Supplementary Material

Refer to Web version on PubMed Central for supplementary material.

## Abbreviations

| | |
|---|---|
| **AB** | antibody |
| **ADM** | acinar-to-ductal metaplasia |
| **ECM** | extracellular matrix |
| **ICAM-1** | intercellular adhesion molecule-1 |
| **MMP** | matrix metalloproteinase |
| **NAB** | neutralizing antibody |
| **PanIN** | pancreatic intraepithelial neoplastic lesion |
| **PDA** | pancreatic ductal adenocarcinoma |
| **TNF** | tumor necrosis factor |

## REFERENCES

1. Hingorani SR, Petricoin EF, Maitra A, Rajapakse V, King C, Jacobetz MA, et al. Preinvasive and invasive ductal pancreatic cancer and its early detection in the mouse. Cancer Cell. 2003; 4:437–450. [PubMed: 14706336]

2. Iacobuzio-Donahue CA. Genetic evolution of pancreatic cancer: lessons learnt from the pancreatic cancer genome sequencing project. Gut. 2012; 61:1085–1094. [PubMed: 21749982]

3. Bardeesy N, DePinho RA. Pancreatic cancer biology and genetics. Nat Rev Cancer. 2002; 2:897–909. [PubMed: 12459728]

4. Guerra C, Collado M, Navas C, Schuhmacher AJ, Hernandez-Porras I, Canamero M, et al. Pancreatitis-induced inflammation contributes to pancreatic cancer by inhibiting oncogene-induced senescence. Cancer Cell. 2011; 19:728–739. [PubMed: 21665147]

5. Dawson DW, Hertzer K, Moro A, Donald G, Chang HH, Go VL, et al. High-fat, high-calorie diet promotes early pancreatic neoplasia in the conditional KrasG12D mouse model. Cancer Prev Res (Phila). 2013; 6:1064–1073. [PubMed: 23943783]

6. Kolodecik T, Shugrue C, Ashat M, Thrower EC. Risk factors for pancreatic cancer: underlying mechanisms and potential targets. Front Physiol. 2013; 4:415. [PubMed: 24474939]

7. Wormann SM, Algul H. Risk Factors and Therapeutic Targets in Pancreatic Cancer. Front Oncol. 2013; 3:282. [PubMed: 24303367]

8. Liou GY, Doppler H, Necela B, Krishna M, Crawford HC, Raimondo M, et al. Macrophage-secreted cytokines drive pancreatic acinar-to-ductal metaplasia through NF-kappaB and MMPs. J Cell Biol. 2013; 202:563–577. [PubMed: 23918941]

9. Ray KC, Moss ME, Franklin JL, Weaver CJ, Higginbotham J, Song Y, et al. Heparin-binding epidermal growth factor-like growth factor eliminates constraints on activated Kras to promote rapid onset of pancreatic neoplasia. Oncogene. 2014; 33:823–831. [PubMed: 23376846]

10. Ardito CM, Gruner BM, Takeuchi KK, Lubeseder-Martellato C, Teichmann N, Mazur PK, et al. EGF receptor is required for KRAS-induced pancreatic tumorigenesis. Cancer Cell. 2012; 22:304–317. [PubMed: 22975374]

11. Ying H, Elpek KG, Vinjamoori A, Zimmerman SM, Chu GC, Yan H, et al. PTEN is a major tumor suppressor in pancreatic ductal adenocarcinoma and regulates an NF-kappaB-cytokine network. Cancer Discov. 2011; 1:158–169. [PubMed: 21984975]

12. Pylayeva-Gupta Y, Lee KE, Hajdu CH, Miller G, Bar-Sagi D. Oncogenic Kras-induced GM-CSF production promotes the development of pancreatic neoplasia. Cancer Cell. 2012; 21:836–847. [PubMed: 22698407]

13. Guerra C, Schuhmacher AJ, Canamero M, Grippo PJ, Verdaguer L, Perez-Gallego L, et al. Chronic pancreatitis is essential for induction of pancreatic ductal adenocarcinoma by K-Ras oncogenes in adult mice. Cancer Cell. 2007; 11:291–302. [PubMed: 17349585]

14. Badiwala MV, Tumiati LC, Joseph JM, Sheshgiri R, Ross HJ, Delgado DH, et al. Epidermal growth factor-like domain 7 suppresses intercellular adhesion molecule 1 expression in response to hypoxia/reoxygenation injury in human coronary artery endothelial cells. Circulation. 2010; 122:S156–S161. [PubMed: 20837907]

15. Whipple CA, Young AL, Korc M. A KrasG12D–driven genetic mouse model of pancreatic cancer requires glypican-1 for efficient proliferation and angiogenesis. Oncogene. 2012; 31:2535–2544. [PubMed: 21996748]

16. Springer TA. Adhesion receptors of the immune system. Nature. 1990; 346:425–434. [PubMed: 1974032]

17. Yang L, Froio RM, Sciuto TE, Dvorak AM, Alon R, Luscinskas FW. ICAM-1 regulates neutrophil adhesion and transcellular migration of TNF-alpha-activated vascular endothelium under flow. Blood. 2005; 106:584–592. [PubMed: 15811956]

18. Hruban RH, van Mansfeld AD, Offerhaus GJ, van Weering DH, Allison DC, Goodman SN, et al. K-ras oncogene activation in adenocarcinoma of the human pancreas. A study of 82 carcinomas using a combination of mutant-enriched polymerase chain reaction analysis and allele-specific oligonucleotide hybridization. Am J Pathol. 1993; 143:545–554. [PubMed: 8342602]

19. Collins MA, Bednar F, Zhang Y, Brisset JC, Galban S, Galban CJ, et al. Oncogenic Kras is required for both the initiation and maintenance of pancreatic cancer in mice. J Clin Invest. 2012; 122:639–653. [PubMed: 22232209]

20. Zheng L, Xue J, Jaffee EM, Habtezion A. Role of immune cells and immune-based therapies in pancreatitis and pancreatic ductal adenocarcinoma. Gastroenterology. 2013; 144:1230–1240. [PubMed: 23622132]

21. Apte MV, Wilson JS, Lugea A, Pandol SJ. A starring role for stellate cells in the pancreatic cancer microenvironment. Gastroenterology. 2013; 144:1210–1219. [PubMed: 23622130]

22. Beatty GL, Chiorean EG, Fishman MP, Saboury B, Teitelbaum UR, Sun W, et al. CD40 agonists alter tumor stroma and show efficacy against pancreatic carcinoma in mice and humans. Science. 2011; 331:1612–1616. [PubMed: 21436454]

23. Liu H, Sidiropoulos P, Song G, Pagliari LJ, Birrer MJ, Stein B, et al. TNF-alpha gene expression in macrophages: regulation by NF-kappa B is independent of c-Jun or C/EBP beta. J Immunol. 2000; 164:4277–4285. [PubMed: 10754326]

24. Mantovani A, Sozzani S, Locati M, Allavena P, Sica A. Macrophage polarization: tumor-associated macrophages as a paradigm for polarized M2 mononuclear phagocytes. Trends Immunol. 2002; 23:549–555. [PubMed: 12401408]

25. Amura CR, Kamei T, Ito N, Soares MJ, Morrison DC. Differential regulation of lipopolysaccharide (LPS) activation pathways in mouse macrophages by LPS-binding proteins. J Immunol. 1998; 161:2552–2560. [PubMed: 9725255]

26. Myers MJ, Pullen JK, Ghildyal N, Eustis-Turf E, Schook LB. Regulation of IL-1 and TNF-alpha expression during the differentiation of bone marrow derived macrophage. J Immunol. 1989; 142:153–160. [PubMed: 2642503]

27. Ahmad R, Raina D, Trivedi V, Ren J, Rajabi H, Kharbanda S, et al. MUC1 oncoprotein activates the IkappaB kinase beta complex and constitutive NF-kappaB signalling. Nat Cell Biol. 2007; 9:1419–1427. [PubMed: 18037881]

28. Masamune A, Sakai Y, Kikuta K, Satoh M, Satoh A, Shimosegawa T. Activated rat pancreatic stellate cells express intercellular adhesion molecule-1 (ICAM-1) in vitro. Pancreas. 2002; 25:78–85. [PubMed: 12131776]

29. Daniluk J, Liu Y, Deng D, Chu J, Huang H, Gaiser S, et al. An NF-kappaB pathway-mediated positive feedback loop amplifies Ras activity to pathological levels in mice. J Clin Invest. 2012; 122:1519–1528. [PubMed: 22406536]

30. Pan X, Arumugam T, Yamamoto T, Levin PA, Ramachandran V, Ji B, et al. Nuclear factor-kappaB p65/relA silencing induces apoptosis and increases gemcitabine effectiveness in a subset of pancreatic cancer cells. Clin Cancer Res. 2008; 14:8143–8151. [PubMed: 19088029]

31. Xiao X, Mruk DD, Cheng CY. Intercellular adhesion molecules (ICAMs) and spermatogenesis. Hum Reprod Update. 2013; 19:167–186. [PubMed: 23287428]

32. Tong S, Neboori HJ, Tran ED, Schmid-Schonbein GW. Constitutive expression and enzymatic cleavage of ICAM-1 in the spontaneously hypertensive rat. J Vasc Res. 2011; 48:386–396. [PubMed: 21464573]

33. Mehner C, Miller E, Khauv D, Nassar A, Oberg AL, Bamlet WR, et al. Tumor Cell-derived MMP-3 Orchestrates Rac1b and Tissue Alterations that Promote Pancreatic Adenocarcinoma. Mol Cancer Res. 2014

34. Van Schaeybroeck S, Kyula JN, Fenton A, Fenning CS, Sasazuki T, Shirasawa S, et al. Oncogenic Kras promotes chemotherapy-induced growth factor shedding via ADAM17. Cancer Res. 2011; 71:1071–1080. [PubMed: 21148749]

35. Tsakadze NL, Sithu SD, Sen U, English WR, Murphy G, D'Souza SE. Tumor necrosis factor-alpha-converting enzyme (TACE/ADAM-17) mediates the ectodomain cleavage of intercellular adhesion molecule-1 (ICAM-1). J Biol Chem. 2006; 281:3157–3164. [PubMed: 16332693]

36. Noh KW, Pungpapong S, Wallace MB, Woodward TA, Raimondo M. Do cytokine concentrations in pancreatic juice predict the presence of pancreatic diseases? Clin Gastroenterol Hepatol. 2006; 4:782–789. [PubMed: 16713745]

37. Shimoyama S, Gansauge F, Gansauge S, Widmaier U, Oohara T, Beger HG. Overexpression of intercellular adhesion molecule-1 (ICAM-1) in pancreatic adenocarcinoma in comparison with normal pancreas. Pancreas. 1997; 14:181–186. [PubMed: 9057191]

38. Roland CL, Dineen SP, Toombs JE, Carbon JG, Smith CW, Brekken RA, et al. Tumor-derived intercellular adhesion molecule-1 mediates tumor-associated leukocyte infiltration in orthotopic pancreatic xenografts. Exp Biol Med (Maywood). 2010; 235:263–270. [PubMed: 20404043]

39. Laheru D, Jaffee EM. Immunotherapy for pancreatic cancer - science driving clinical progress. Nat Rev Cancer. 2005; 5:459–467. [PubMed: 15905855]

40. Bausch D, Thomas S, Mino-Kenudson M, Fernandez-del CC, Bauer TW, Williams M, et al. Plectin-1 as a novel biomarker for pancreatic cancer. Clin Cancer Res. 2011; 17:302–309. [PubMed: 21098698]

41. Burns RC, Rivera-Nieves J, Moskaluk CA, Matsumoto S, Cominelli F, Ley K. Antibody blockade of ICAM-1 and VCAM-1 ameliorates inflammation in the SAMP-1/Yit adoptive transfer model of Crohn's disease in mice. Gastroenterology. 2001; 121:1428–1436. [PubMed: 11729122]

42. Iigo Y, Takashi T, Tamatani T, Miyasaka M, Higashida T, Yagita H, et al. ICAM-1-dependent pathway is critically involved in the pathogenesis of adjuvant arthritis in rats. J Immunol. 1991; 147:4167–4171. [PubMed: 1684374]

43. Patel SS, Thiagarajan R, Willerson JT, Yeh ET. Inhibition of alpha4 integrin and ICAM-1 markedly attenuate macrophage homing to atherosclerotic plaques in ApoE-deficient mice. Circulation. 1998; 97:75–81. [PubMed: 9443434]

44. Vuorte J, Lindsberg PJ, Kaste M, Meri S, Jansson SE, Rothlein R, et al. Anti-ICAM-1 monoclonal antibody R6.5 (Enlimomab) promotes activation of neutrophils in whole blood. J Immunol. 1999; 162:2353–2357. [PubMed: 9973515]

45. Jackson EL, Willis N, Mercer K, Bronson RT, Crowley D, Montoya R, et al. Analysis of lung tumor initiation and progression using conditional expression of oncogenic K-ras. Genes Dev. 2001; 15:3243–3248. [PubMed: 11751630]

46. Mohammed A, Janakiram NB, Li Q, Madka V, Ely M, Lightfoot S, et al. The epidermal growth factor receptor inhibitor gefitinib prevents the progression of pancreatic lesions to carcinoma in a conditional LSL-KrasG12D/+ transgenic mouse model. Cancer Prev Res (Phila). 2010; 3:1417–1426. [PubMed: 21084261]

47. Nakhai H, Sel S, Favor J, Mendoza-Torres L, Paulsen F, Duncker GI, et al. Ptf1a is essential for the differentiation of GABAergic and glycinergic amacrine cells and horizontal cells in the mouse retina. Development. 2007; 134:1151–1160. [PubMed: 17301087]

48. Mook OR, Van Overbeek C, Ackema EG, Van Maldegem F, Frederiks WM. In situ localization of gelatinolytic activity in the extracellular matrix of metastases of colon cancer in rat liver using quenched fluorogenic DQ-gelatin. J Histochem Cytochem. 2003; 51:821–829. [PubMed: 12754293]

49. Means AL, Meszoely IM, Suzuki K, Miyamoto Y, Rustgi AK, Coffey RJ Jr, et al. Pancreatic epithelial plasticity mediated by acinar cell transdifferentiation and generation of nestin-positive intermediates. Development. 2005; 132:3767–3776. [PubMed: 16020518]

50. Esni F, Miyamoto Y, Leach SD, Ghosh B. Primary explant cultures of adult and embryonic pancreas. Methods Mol Med. 2005; 103:259–271. [PubMed: 15542912]

## STATEMENT OF SIGNIFICANCE

We here show that oncogenic Kras in pancreatic acinar cells upregulates the expression of ICAM-1 to attract macrophages. Hence, our results reveal a direct cooperative mechanism between oncogenic Kras mutations and the inflammatory environment to drive the initiation of pancreatic cancer.
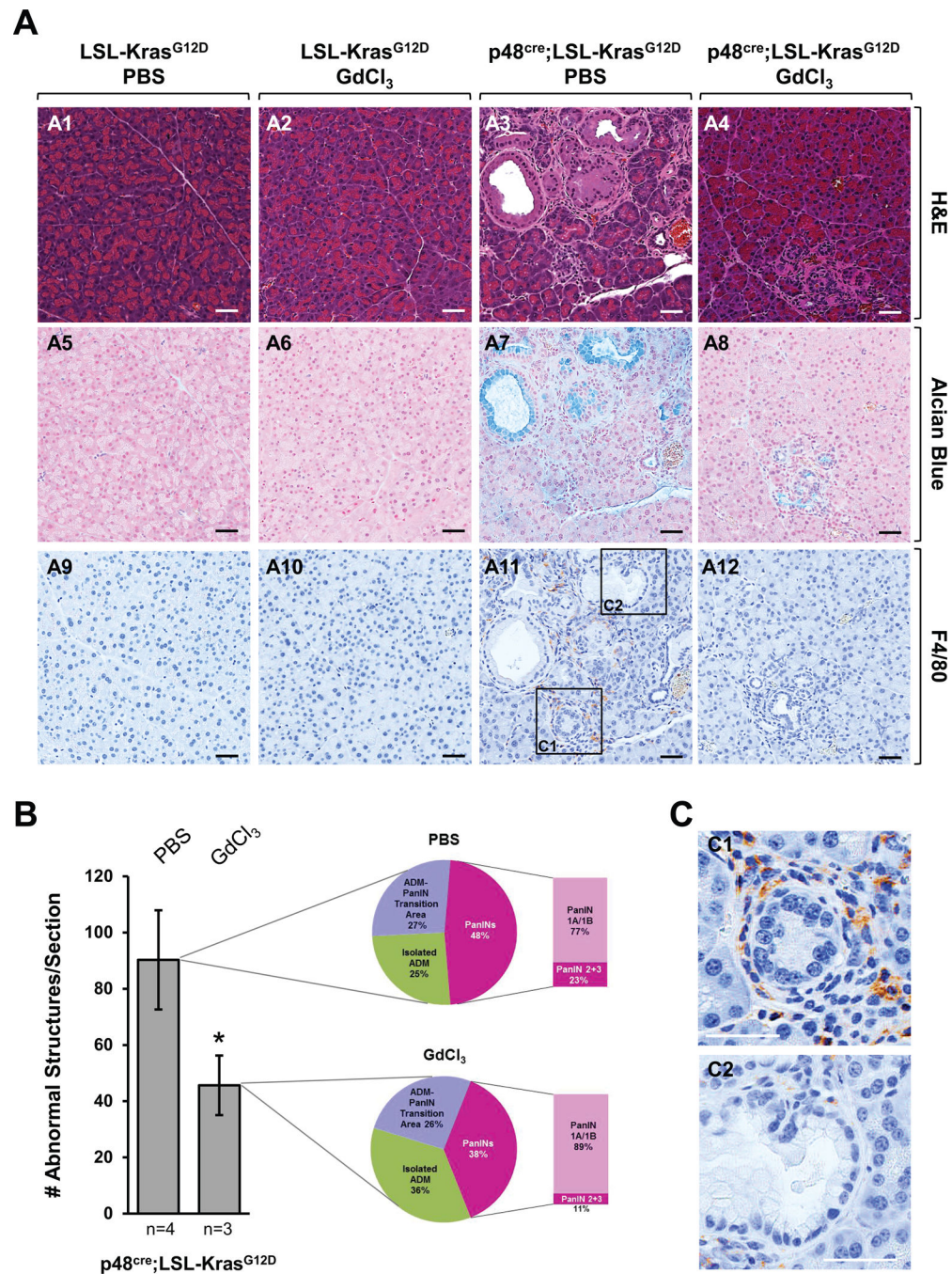
**Fig. 1. Depletion of macrophages attenuates progression of Kras-caused abnormal structures**
(**A–C**) At seven weeks of age, p48$^{cre}$;LSL-Kras$^{G12D}$ mice (or control mice; shown are LSL-Kras$^{G12D}$) were injected with GdCl$_3$ or PBS as indicated. GdCl$_3$ (10 mg/kg) was intravenously-injected through the tail vein every 2 days for 1 week. After a two week rest animals were treated a second time with GdCl$_3$ every 2 days for 1 week (treatment scheme outlined in Supplemental Figure S1A). At the endpoint (week 13) pancreata were harvested and analyzed. (**A**) Pancreata were subjected to IHC for H&E, alcian blue and F4/80. A representative area of the pancreas tissue is shown. The scale bar is 50 μm. (**B**) H&E stained

tissue samples from PBS- (n=4) or GdCl$_3$-treated (n=3) p48$^{cre}$;LSL-Kras$^{G12D}$ mice were evaluated and quantitated for abnormal structures. Bar graph: Quantitation of abnormal structures (isolated ADM regions, ADM-PanIN transition areas and PanIN lesions all combined) per pancreas section. Pie graphs: Percentage of isolated ADM areas, ADM-PanIN transition areas and PanINs. **(C)** Enlarged sections of an ADM area (C1) and a PanIN1 lesion (C2) from F4/80 staining. The scale bar is 50 μm.
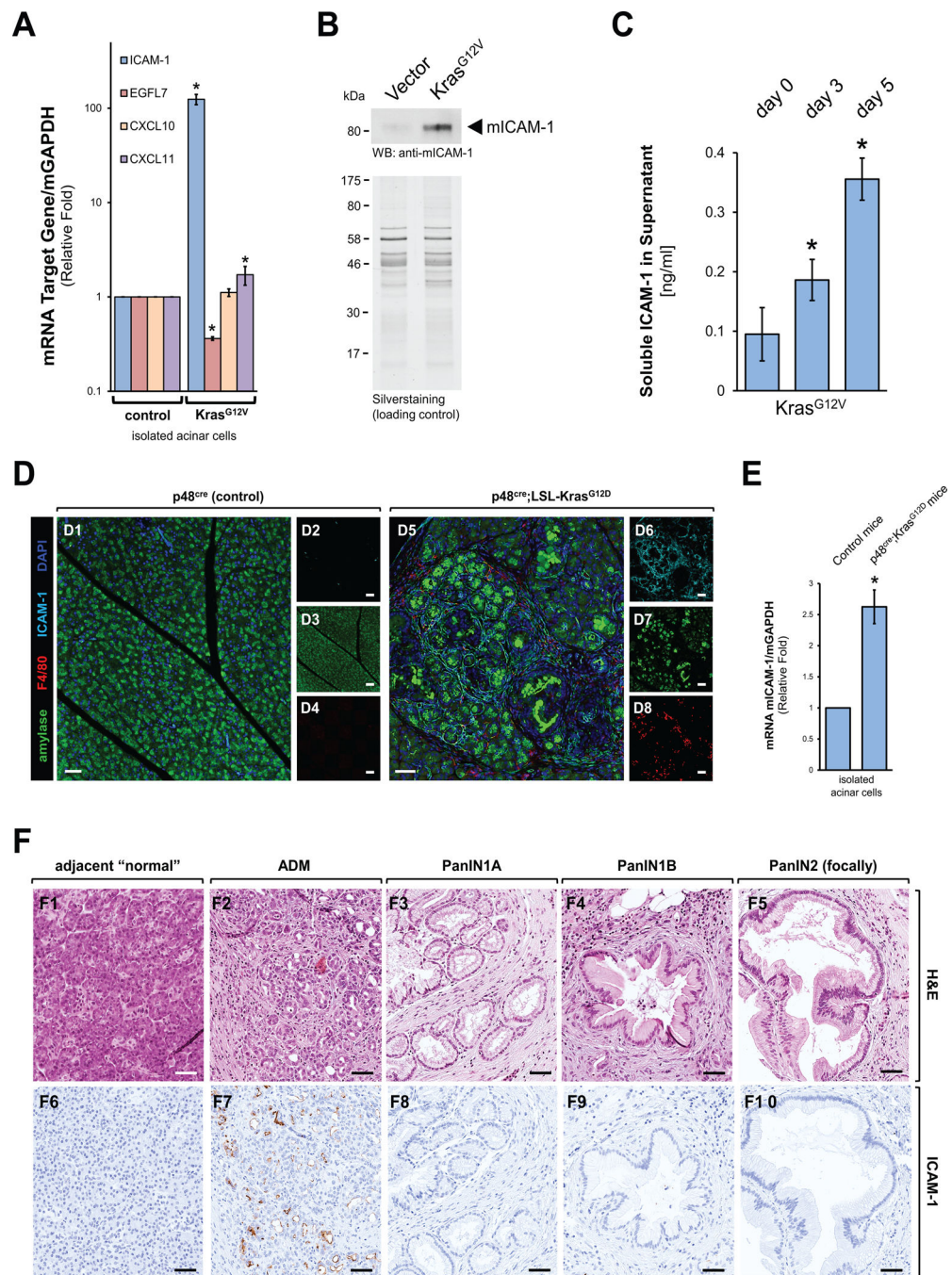
**Fig. 2. Mutant Kras induces expression of ICAM-1 in acinar cells**

(A–C) Mouse primary pancreatic acinar cells were isolated, infected with lentivirus carrying an oncogenic Kras (Kras[G12V]) mutant and seeded in 3D organoid culture. After 5 days, cells were analyzed for expression of ICAM1, CXCL10, CXCL11 or EGFL7 using quantitative PCR (A), for expression of ICAM1 using Western blot (B; silver staining served as loading control). In addition, at days 0, 3 and 5 of Kras[G12V] expression, supernatants were analyzed by ELISA for soluble ICAM-1 (C). (D) Pancreata of p48[cre];LSL-Kras[G12D] or control (shown is p48[cre]) mice at week 14 were analyzed for expression of ICAM1, macrophage

infiltration (F4/80) and amylase expression (acinar cell marker) using immunofluorescence labeling. DAPI marks the nuclei. Left side shows composite and right side single channels. The bar indicates 50 μm. **(E)** Acinar cells were isolated from 6 weeks old p48[cre];LSL-Kras[G12D] or control (shown is p48[cre]) mice and analyzed for expression of ICAM1 using quantitative PCR. **(F)** Human tissue samples with regions of ADM or PanIN1A, PanIN1B, or PanIN2 (focally) lesions were stained with H&E (top row) or ICAM1 (IHC, bottom row). The bar indicates 50 μm.
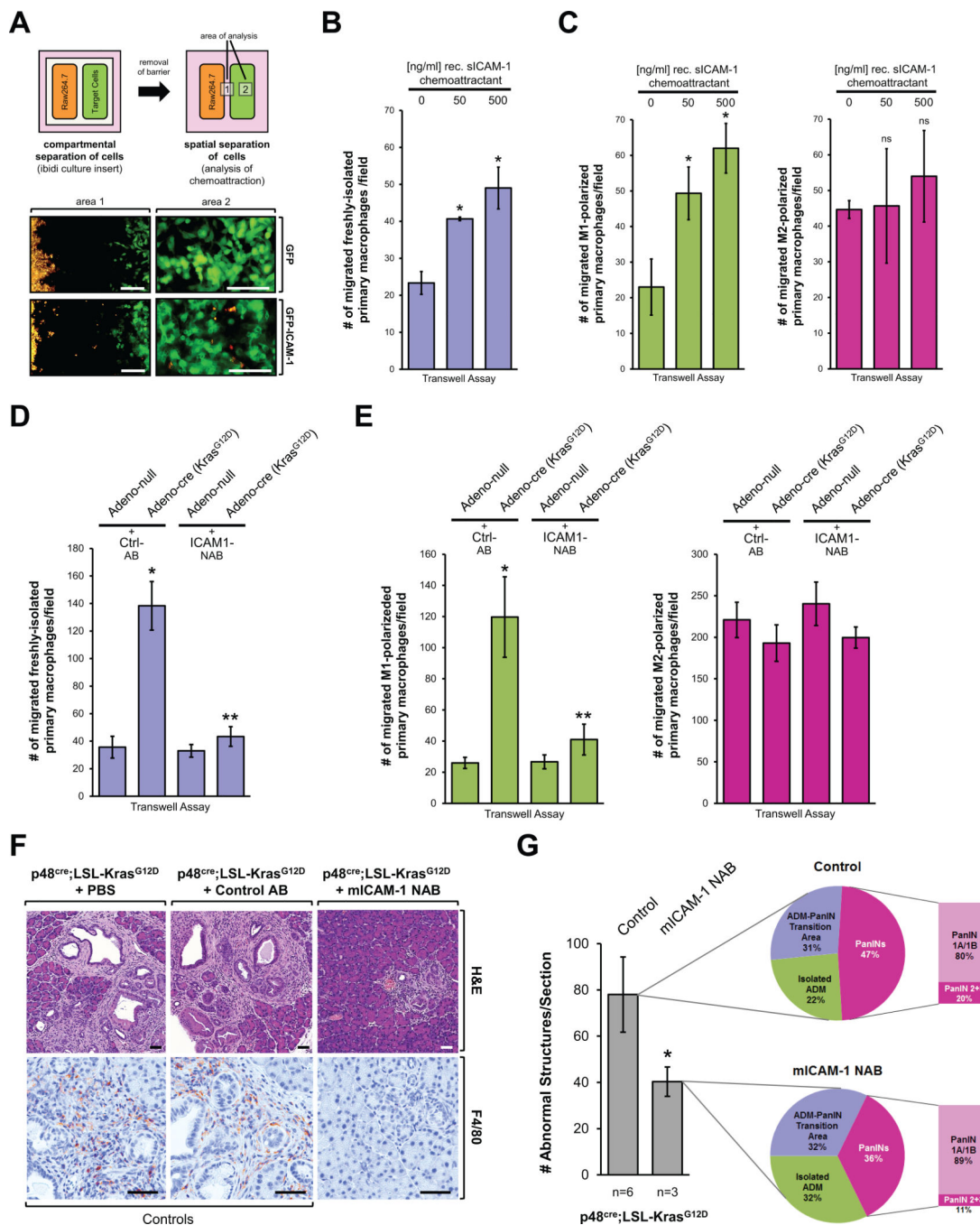
**Fig. 3. Kras induced chemoattractants mediate attraction of macrophages**

(**A**) $7 \times 10^4$ HeLa cells stably-expressing either GFP or GFP-tagged full-length transmembrane ICAM-1, and $7 \times 10^4$ DiI-labeled Raw264.7 cells were plated as indicated in an ibidi removable 2 well silicone culture insert that was placed in a cell culture μ-Dish. 24 hours after seeding the culture inserts were carefully removed. After 24 hours, migration of macrophages towards HeLa-GFP or HeLa-GFP-ICAM-1 cells was assessed by fluorescent microscopy in indicated areas 1 and 2. The bar indicates 200 μm. (**B, C**) Freshly-isolated primary mouse macrophages (B), or M1 or M2 polarized primary mouse macrophages (C)

were seeded in a Transwell chamber and migration towards recombinant ICAM1 (0, 50, 500 ng/ml) was determined (t = 16 hours). Shown are numbers of migrated macrophages per field. The asterisk indicates statistical significance as compared to the control. (**D, E**) Primary mouse pancreatic acinar cells from LSL-Kras$^{G12D}$ mice were isolated and infected with adeno-null virus (control) or adenovirus harboring *cre* recombinase to induce expression of oncogenic Kras. Cells were then seeded in bottom wells of transwell chambers. Live dye-labeled freshly-isolated primary mouse macrophages (D), or M1 or M2 polarized primary mouse macrophages (E) were added into the top chambers of the Transwell plates and migration towards the acinar cells was determined either in presence of isotype-matched control antibody (Ctrl-AB) or an ICAM-1 neutralizing antibody (NAB). Shown are numbers of migrated macrophages per field. * indicates statistical significance as compared to the adeno-null control; ** indicates statistical significance as compared to Adeno-cre. (**F**) At three weeks of age, p48$^{cre}$;LSL-Kras$^{G12D}$ mice (or control mice; **see** Supplemental Fig. S5A) were injected every other day with ICAM-1 neutralizing antibody (NAB), isotype-matched control antibody (Control AB) or vehicle control (PBS) for a total of 11 weeks. Pancreata were subjected to IHC for H&E and F4/80. A representative area of the pancreas tissue under each condition is shown. Scale bar is 50 μm. (**G**) H&E stained tissue samples from control (n=6) or mICAM-1 NAB-treated (n=3) p48$^{cre}$;LSL-Kras$^{G12D}$ mice were evaluated and quantitated for abnormal structures. Bar graph: Quantitation of abnormal structures (isolated ADM regions, ADM-PanIN transition areas and PanIN lesions all combined) per section. Pie graphs: Percentage of isolated ADM areas, ADM-PanIN transition areas and PanINs.

**Fig. 4. Presence of TNF and ECM degradation are consequences of abundance of macrophages in regions of ADM**

(**A**) Pancreata of p48^cre;LSL-Kras^G12D treated with PBS or mICAM-1 NAB (see Figure 3D) were analyzed for expression of TNF in regions of macrophage infiltration using immunofluorescence labeling. F4/80 marks macrophages and DAPI marks the nuclei. Left side shows composite and right side single channels. The bar indicates 100 μm. (**B**) Primary mouse pancreatic acinar cells from LSL-Kras^G12D mice were isolated and infected with adeno-null virus (control) or adenovirus harboring *cre* recombinase to induce expression of

mutant Kras (labeled: Kras$^{G12D}$). Cells then were seeded in 3D *explant* organoid culture in absence (control) or presence of recombinant mouse TNF (50 ng/ml). ADM events were determined at day 5. Bar graph: * indicates statistical significance as compared to the control (adeno-null + control treatment), ** indicates statistical significance to control and to TNF-treated adeno-null group; *** indicates statistical significance to all other groups. Photos show representative areas of the explant culture. The bar is 200 μm. **(C)** Pancreata of p48$^{cre}$;LSL-Kras$^{G12D}$ mice were subjected to *in situ* zymography followed by DAPI staining as described in materials & methods. The scale bar is 25 μm. **(D)** Pancreata of p48$^{cre}$;LSL-Kras$^{G12D}$ mice (or control mice; shown are LSL-Kras$^{G12D}$) injected with GdCl$_3$ or PBS as indicated in Supplemental Figure S1A were subjected to H&E staining and immunofluorescence analysis for F4/80 and MMP9. DAPI stain was added to visualize nuclei. A representative area of the pancreas tissue is shown. The scale bar is 50 μm. **(E)** Scheme of how Kras$^{G12D}$-expressing acini and M1-polarized macrophages may crosstalk to potentiate acinar-to-ductal metaplasia.